International Journal of Advances in Bio-Informatics and Bio-Technology – IJABB
Volume 1 : Issue 1 [ISSN 2475-2258]
Publication Date : 25 June 2014

Biomimetic Design of Protein Microspheres

Sungkwon Yoon, William T. Nichols*

***Abstract*—Living cells in our body present striking complex structures and functions. Inspired by this, biomimetic design approaches for protein microspheres are discussed. The protein microspheres are synthesized using an ultrasonic method. Size control and surface morphology modification is achieved by modulating experimental parameters. The concentration of protein changes the size of microspheres. Different internal oil phase defines the morphology of surface. Nanoparticles are embedded inside and outside of the microspheres, yielding nano-functionalization. Self-assembly for complex structures is also introduced using microspheres as build blocks. The designed microspheres and assembled structures are envisioned to have applications in biomedical, catalyst, and materials sciences.**

***Keywords*—Protein microspheres, Sonochemistry, Ultrasonic, Biomimetics, Colloidal self-assembly**

I. Introduction

Living organisms are composed of fundamental units, the cells. These tiny but amazingly complex entities handle all the events and issues that occur in life. Cells process and produce matter and energy. They respond, sense, and communicate dynamically to their environment. Mimicking this feature enables us to create highly functional microsystems. Furthermore, we can expect to have diverse macrostructures by assembling these units just as cells build tissues, organs, and our body.

In 1990, Suslick and Grinstaff developed a procedure for making protein microspheres by ultrasonic irradiation [1]. According to the mechanism, an oil phase is emulsified into the protein aqueous solution by ultrasonic energy. Subsequently, the protein molecules polymerize on the oil droplets through disulfide linkages. This protein microsphere is hollow, and has the protein shell which can hold functionalities. It also has micrometer sizes similar to biologicial cells.

Here we report biomimetic approaches to design protein microspheres. We take inspiration from living cells and apply these concepts to create properties. Size control, surface modification, and nano-functionalization are achieved by modulating parameters in the synthetic procedure. Moreover, we demonstrate some assembly techniques of complex structures using protein microspheres. Colloidal self-assemblies of porous scaffolds, monolayers, anisotropic aggregations, and fibers are studied with protein microspheres as building blocks.

Sungkwon Yoon, William T. Nichols
Division of Materials Science and Engineering, Hanyang University
Seoul, South Korea

II. Experimental

Protein microspheres were synthesized as described previously [1]. The protein bovine serum albumin (BSA, Sigma Aldrich) and *n*-dodecane (Kanto Chemical) were used as received. In a typical method, 6.7 ml of *n*-dodecane was carefully layered on the 10 ml of aqueous BSA protein solution (0.1 to 5 w/v %). A high intensity ultrasonic energy was introduced at the oil and water interface by a horn-type irradiator (Vibra-Cell VS-750, Sonics and Materials). The sonication was carried out for 3 minutes at 560 W. The temperature of the solution was maintained below 30 °C with an ice bath to avoid unintended protein denaturation. After synthesis, microspheres were separated from excess protein by 5 cycles of centrifugation (1000 g, 10 min). The analysis of the microspheres was performed by optical microscopy, SEM, FESEM, TEM-EDS, and dynamic light scattering (DLS, Zetasizer Nano ZS, Malvern instruments).

To make porous scaffolds, a 7 ml of aliquot of purified microspheres was freeze-dried in a small petri dish. The specific surface area was measured by Brunauer-Emmett-Teller (BET) analysis after N2 sorption with Micromeritics TriStar II 3020.

For monolayer assembly, microspheres were cross-linked together by the following steps. Purified protein microspheres were dispersed in 0.1 M of sodium chloride aqueous solution. The fixative, glutaraldehyde (Sigma Aldrich), was then added to the solution. White layers started to form on the water surface after 15 minutes. The sample was collected carefully using an optical cover glass.

To control the surface morphology of microspheres, a total of three different oil phases including *n*-dodecane, toluene, and chloroform were used as the internal oil phase. The experimental procedure followed a standard routine as mentioned above. The surface morphology of microspheres was studied by atomic force microscopy (AFM, XE-100, Park Systems).

Gold nanoparticles were prepared with the trisodium citrate reduction method as reported without modifications [2]. BSA protein was dissolved in the gold nano-sol instead of pure water. Synthesis of microspheres was the same process as described above.

Magnetite nanoparticles (25 nm in diameter, Sigma Aldrich) were dispersed at 0.9 w/v % in corn oil. This ferrofluid was used as the oil phase in the standard method. The resulting microspheres were studied by vibrating sample magnetometry (VSM, 7304, LakeShore) to determine the magnetization. Fibrous assembly of the magnetic microspheres was accomplished by a permanent magnet with surface field of 3580 G.

III. Results and discussion

A. *Effects of protein concentration*

The size of biological cells varies quite a lot depending on their function. Skin cells average about 50 micrometers. Red blood cells are smaller, usually falling in a range of 6 to 8 micrometers in order to provide smooth passage through the blood vessels [3]. Each cell has an optimized size about its spatial area. By mimicking this feature, we studied the ability to control our microsphere size to make them adaptable to changes in various dimensions.

The typical emulsion system provides controllability of droplet size through a surfactant [4-5]. Our synthetic method for protein microspheres relies on oil in water ultrasonic emulsification having BSA protein as surfactant. Figure 1 shows the result of the microsphere size versus protein concentration. It is seen that decreasing concentration from 5 w/v % to 0.1 w/v % makes increasing mean diameter from 2.5 μm to 22.5 μm (left graph). DLS study (right graph) for 5 w/v % and 1 w/v % also presents the increasing trend in mean diameters. Optical microscopic images in the bottom row show the actual images for some conditions. The microspheres are well dispersed and uniformly spherical. From DLS analysis and images, we can see microspheres are not monodisperse. This polydispersity is nonetheless valuable to assemble complex structures as discussed below.

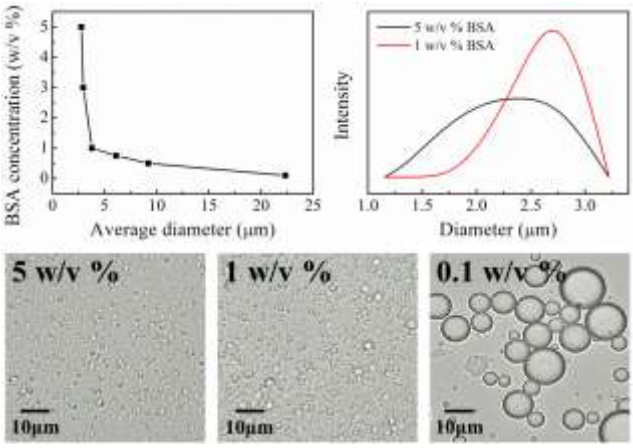

Figure 1. Mean size distribution of protein microspheres prepared from various protein concentrations (upper-left). DLS size measurements for 1 w/v % and 5 w/v % (upper-right). Optical microscopic images showing microspheres from several concentrations (bottom row).

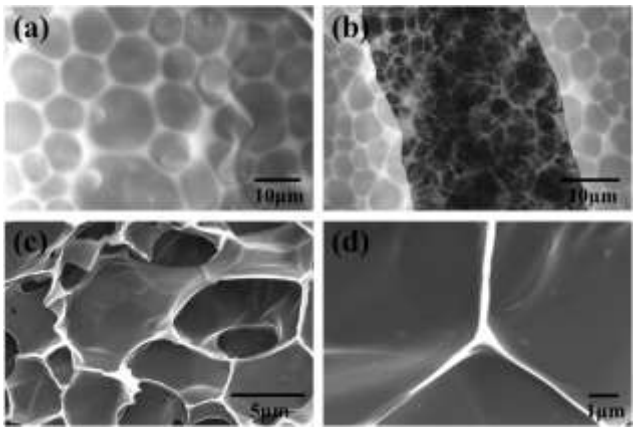

Figure 2. SEM images for (a) palletized protein microspheres, (b) an open gap, (c) a cross sectional image from the open gap, and (d) a higher magnification image shows shape deformation in tightly packed microspheres.

Centrifuged and palletized protein microspheres are shown in Figure 2(a). We can see how microspheres are packed together. The small microspheres locate in the spaces between larger ones, increasing the packing density [6]. In addition, Protein microspheres are not rigid spheres. We can see the cross-sectional images from an open gap in Figure 2(b). Deformation in their shape is possible from spherical to various elongated or polyhedral shapes to promote tighter packing as shown in Figure 2(c, d). By expanding this idea, three different self-assemblies are achieved.

Figure 3(a) shows the protein porous scaffold. Freeze-drying was introduced to remove outside water media and the internal oil phase. Water dehydration occurs, so the microspheres are packed tightly by capillary force. The internal *n*-dodecane escapes through small cracks in the 30 nm thick protein shell maintaining spherically shaped pores. The scaffold has a feeling like cotton, light-weight, and self-supporting. BET analysis shows these scaffolds have a high specific surface area of 28.1 m^2/g.

The as synthesized microspheres are buoyant in water due to their low density internal oil phase. The microspheres monolayer is prepared using this property. Cross-linked

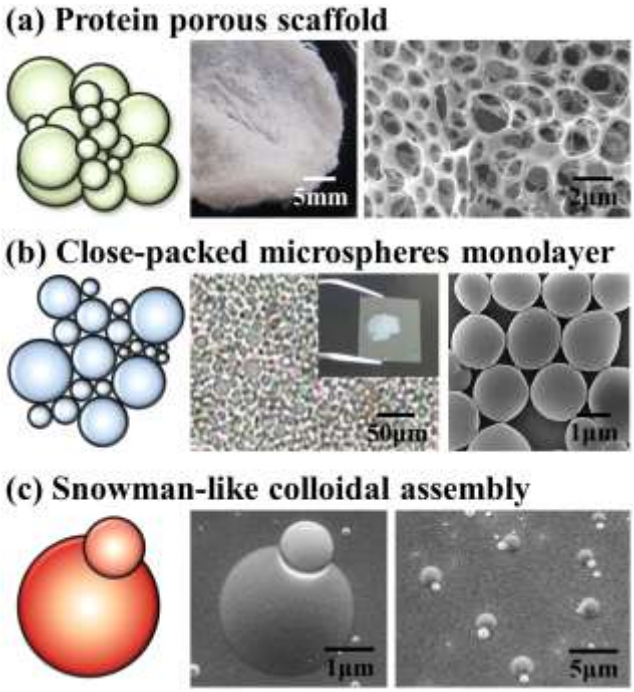

Figure 3. Self-assembly in protein microspheres; (a) a protein porous

scaffold from freeze-drying concentrated microspheres, (b) a monolayer made by close-packed microspheres, and (c) snowman-like colloidal self-assemblies.

microspheres with glutaraldehyde form close-packing layers on the water surface. The monolayer is carefully peeled off onto a glass substrate as seen in Figure 3(b). They are closely packed, although we can notice less deformation of spherical shape due to less external stress compare to the previous cases.

Some interesting anisotropic aggregations are also observed. We can see the snowman-like colloidal assembly in Figure 3(c). Differently sized microspheres formed naturally in an ultrasonic reactor are deformed and attached strongly together. These kinds of assembly techniques may lead to interesting applications like bio-tissue scaffolds, membranes, filters, and biocatalysts.

B. *Effects of internal oil phase*

In a previous study, toluene was used as the internal oil phase and made protein microspheres with a rough surface [7]. The solubility between water and oil was indicated as a key factor for this phenomenon. The surface roughness versus solubility of oil in water was studied by AFM. The following three different oily liquids are used as the oil phase in ultrasonic synthesis; *n*-dodecane, toluene, and chloroform. Each liquids have the solubility in water of 0.000037, 0.052, and 0.82 (w/w %) respectively [8-9]. Surface morphology information of the resulting microspheres is shown in Figure 4. The graph shows the calculated roughness parameters. We can see the microsphere with *n*-dodecane has smooth surface, whereas toluene and chloroform filled microspheres have bumpy surfaces. Strong surface tension at the interface between *n*-dodecane and water results in the smooth surface. In the case of toluene and chloroform, however, more solubility makes an unstable interface between oil and water. Due to this interface instability, the Rayleigh instability, random perturbations at the interface can persist without damping [10]. The perturbations in turn produce rough surfaces on the protein microspheres.

We can now think about the possible applications inspired from biology. Cells are not perfectly spherical and smooth.

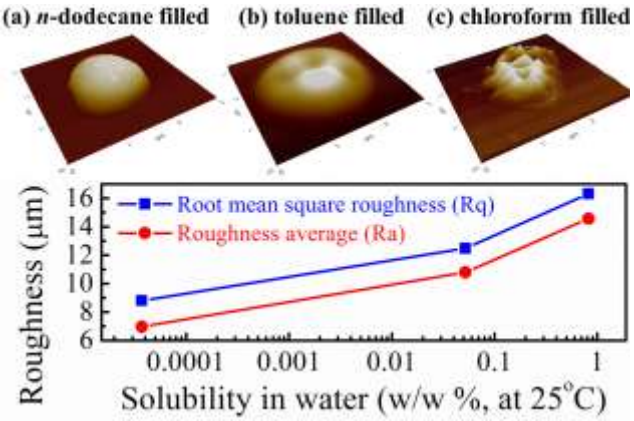

Figure 4. AFM analysis for protein microspheres with three different internal oil phases.

For instance, Golgi apparatus activates protein delivery through increased surface roughness [3]. Dendritic cells maximize surface area by its dendrites to catch pathogens better. Similarly, we can modulate the surface property of protein microsphere by controlling surface morphology which is important for catalyst engineering.

C. *Effects of additives*

Cells have nano-sized particles, tubes, sheets, pods, and cages inside and outside. They support cellular functions by acting as receptors, channels, reaction sites, and binding sites [11]. Inspired by this, we designed two experiments to explore the possibility of adding nanoparticles into microspheres.

First, gold nanoparticles are added in the water phase. Fig. 5 photographs show the pristine protein microspheres (left), and the microspheres with gold (right). The color of microsphere solution is changed due to the red color of the gold nanoparticles. A TEM image is shown on the right side of the photographs. We can see a dim circle presenting a protein microsphere, and black dots of gold nanoparticles. BSA protein is known to have a spontaneous gold-sulfur covalent interaction [12-13]. From the EDS mapping images on the bottom row, we can notice that gold nanoparticles are anchored on the BSA protein shell by the Au-S bonds. The ability to embed nanoparticles on the shell of microspheres opens up applications such as biosensors, biocatalysts, and specific adsorption studies.

For the second experiment, magnetite nanoparticles are dispersed in corn oil. The carboxylic groups in fatty acid molecules are known to anchor on the surface of magnetite.

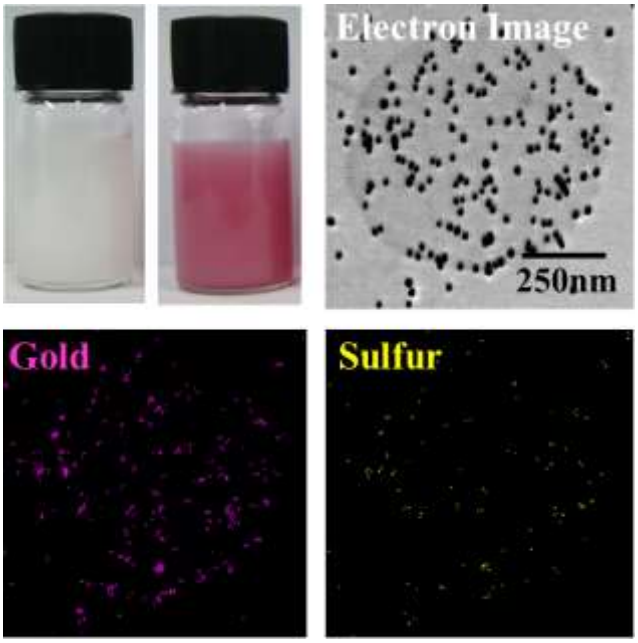

Figure 5. The photographs and TEM-EDS study show the gold nanoparticle embedded protein microspheres.

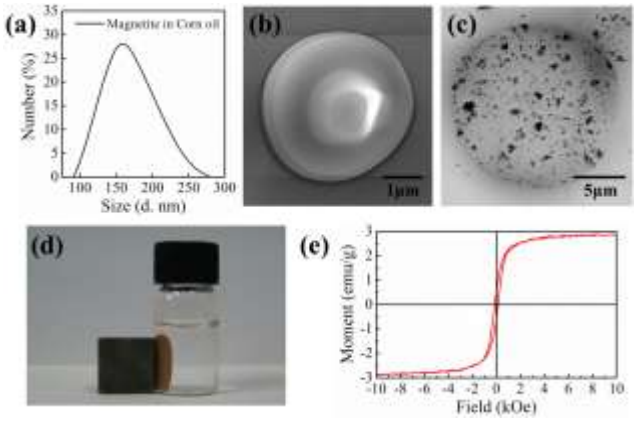

Figure 6. (a) Dispersion state of magnetite nanoparticles in corn oil. (b) SEM image of resulting microspheres with magnetite. (c) TEM image of microsphere encapsulating magnetite nanoparticles. (d) Photograph shows magnetic microspheres responding to an external magnet. (e) Magnetization curve of the magnetic microspheres.

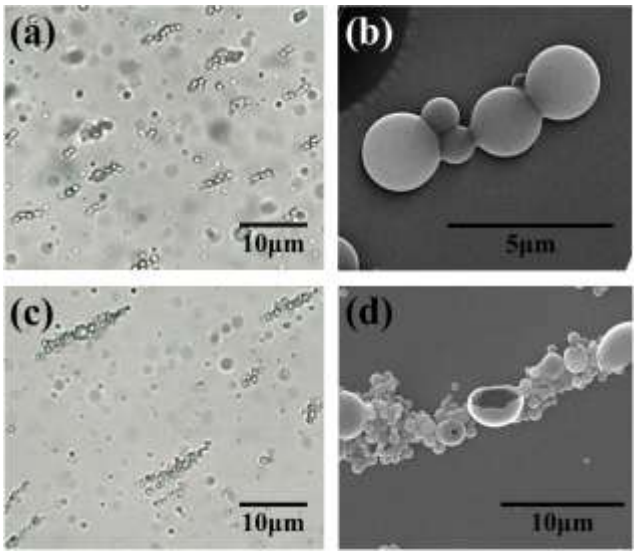

Figure 7. Fibrous assemblies of magnetic protein microspheres.

The alkyl chains make the particle surfaces lipophilic [14]. DLS measurement shows the magnetite nanoparticles are well dispersed in corn oil with a Gaussian distribution (Figure 6(a)). Figure 6(b, c) shows the resulting microspheres. We can see nanoparticles are encapsulated with in the protein shell. These magnetic microspheres respond easily to an external magnet as seen in Figure 6(d). VSM measurements show a magnetization of 3 emu/g (Figure 6(e)).

We discovered a directed colloidal assembly using the magnetic property. Figure 7(a, b) shows magnetic microspheres aligned into fibers. The length of fibers can be increased with a higher concentration of microspheres in water as we can see in Figure 7(c, d). This external control of the microspheres enables us to have potential applications in the targeted drug delivery system, bio-signal tracking, and microfluidic devices.

IV. Conclusions

We presented how to design protein microspheres from the biomimetic point of view. First, the size of microspheres can be controlled by the concentration of protein. Furthermore, polydispersity in size and deformation in shape lead the various structures such as the porous scaffold, monolayer film, and anisotropic self-assembly. Second, surface morphology modification is achieved. It was studied with AFM analysis that increasing solubility between water and oil phase makes the rougher surface of microspheres. Third, simple methods to embed nanoparticles are discovered using both water and oil phases. The gold nanoparticles were anchored on the surface by the Au-S covalent interaction. The magnetite nanoparticles were encapsulated in microspheres, resulting magnetic functionalization.

The research is now aiming at mimicry of the materials transport mechanism into and out of cells. A long term goal is to apply these designs to such as sensors, catalysts, and tissue scaffolds.

Acknowledgment

This work was supported by the National Research Foundation of Korea (NRF) grant funded by the Korean government (MSIP) (No. 2011-0013704) and the research fund of Hanyang University (HY-2010-N).

References

[1] K. S. Suslick, and M. W. Grinstaff, "Protein microencapsulation of nonaqueous liquids," J. Am. Chem. Soc., vol. 112, pp. 7807–7809, 1990

[2] N. Nath, and A. Chilkoti, "A colorimetric gold nanoparticle sensor to interrogate biomolecular interactions in real time on a surface," Anal. Chem., vol. 74, pp. 504–509, 2002

[3] D. Krogh, Biology: A guide to the natural world, 5th ed., Pearson, California, 2010

[4] J. P. Canselier, H. Delmas, A. M. Wilhelm, and B. Abismail, "Ultrasound emulsification–An overview," J. Dispersion. Sci. Tech., vol. 23, pp. 333–349, 2002

[5] S. Tcholakova, N. D. Denkov, and T. Danner, "Role of surfactant type and concentration for the mean drop size during emulsification in turbulent flow," Langmuir, vol. 20, pp. 7444–7458, 2004

[6] D. Myers, Surfaces, Interfaces, and Colloids: Principles and Applications, 2nd ed., Wiley-VCH, New York, 1999

[7] K. Makino, T. Mizorogi, S. Ando, T. Tsukamoto, and H. Ohshima, "Sonochemically prepared bovine serum albumin microcapsules: factor affecting the size distribution and the microencapsulation yield," Colloid. Surface. B., vol. 22, pp. 251–255, 2001

[8] D. G. Shaw, A. Maczynski, M. Goral, B. Wisniewska-Goclowska, A. Skrzecz, I. Owczarek, K. Blazej, M. C. Haulait-Pirson, G. T. Hefter, F. Kapuku, Z. Maczynska, and A. Szafranski, "IUPAC-NIST Solubility Data Series. 81. Hydrocarbons with Water and Seawater - Revised and Updated. Part 10. C_{11} and C_{12} Hydrocarbons with Water," J. Phys. Chem. Ref. Data, vol. 35, No. 1, pp. 153–203, 2006

[9] I. M. Smallwood, Handbook of Organic Solvent Properties, Elsevier, Amsterdam, 1996

[10] S. Chandrasekhar, Hydrodynamic and Hydromagnetic Stability, Dover Publications, New York, 1981

[11] S. Mann "Life as a nanoscale phenomenon," Angew. Chem. Int. Edit., vol. 47, pp. 5306–5320, 2008

[12] T. H. L. Nghiem, T. H. La, X. H. Vu, V. H. Chu, T. H. Nguye n, Q. H. Le, E. Fort, Q. H. Do, and H. N. Tran, "Synthesis, capping and binding of colloidal gold nanoparticles to proteins," Adv. Nat. Sci.: Nanosci. Nanotechnol., vol. 1, pp. 025009, 2010

[13] M.-L. Cui, J.-M. Liu, X.-X. Wang, L.-P. Lin, L. Jiao, L.-H. Zhang, Z.-Y. Zheng, and S.-Q. Lin, "Selective determination of cysteine using BSA-stabilized gold nanoclusters with red emission," Analyst, vol. 137, pp. 5346–5351, 2012

[14] L. Zhang, R. He, and H.-C. Gu, "Oleic acid coating on the monodisperse magnetite nanoparticles," Appl. Surf. Sci., vol. 253, pp. 2611–2617, 2006